© 2015. Published by The Company of Biologists Ltd | Journal of Cell Science (2015) 128, 1375–1385 doi:10.1242/jcs.162925

RESEARCH ARTICLE

# The Arf and Rab11 effector FIP3 acts synergistically with ASAP1 to direct Rabin8 in ciliary receptor targeting

**Jing Wang[1] and Dusanka Deretic[1,2,*]**

## ABSTRACT

Primary cilia have gained considerable importance in biology and disease now that their involvement in a wide range of human ciliopathies has been abundantly documented. However, detailed molecular mechanisms for specific targeting of sensory receptors to primary cilia are still unknown. Here, we show that the Arf and Rab11 effector FIP3 (also known as RAB11FIP3) promotes the activity of Rab11a and the Arf GTPase-activating protein (GAP) ASAP1 in the Arf4-dependent ciliary transport of the sensory receptor rhodopsin. During its passage out of the photoreceptor Golgi and trans-Golgi network (TGN), rhodopsin indirectly interacts with FIP3 through Rab11a and ASAP1. FIP3 competes with rhodopsin for binding to ASAP1 and displaces it from the ternary complex with Arf4–GTP and ASAP1. Resembling the phenotype resulting from lack of ASAP1, ablation of FIP3 abolishes ciliary targeting and causes rhodopsin mislocalization. FIP3 coordinates the interactions of ASAP1 and Rab11a with the Rab8 guanine nucleotide exchange factor Rabin8 (also known as RAB3IP). Our study implies that FIP3 functions as a crucial targeting regulator, which impinges on rhodopsin–ASAP1 interactions and shapes the binding pocket for Rabin8 within the ASAP1–Rab11a–FIP3 targeting complex, thus facilitating the orderly assembly and activation of the Rab11–Rabin8–Rab8 cascade during ciliary receptor trafficking.

**KEY WORDS: Cilium, Rab11a, Rhodopsin**

## INTRODUCTION

Nearly all eukaryotic cells contain exquisitely organized membrane projections called primary cilia that are contiguous with, yet separated from, the surrounding plasma membrane by the periciliary diffusion barrier, which gives them properties of a separate organelle. Primary cilia function as environmental sensors that capture a wide range of extracellular signals through sensory receptors and their associated signal transduction machineries, which are highly concentrated in the ciliary membrane (Singla and Reiter, 2006). The strict compartmentalization of the sensory membranes is achieved by the directed transport of signaling molecules to the base of the cilia, followed by the selective admission through the periciliary diffusion barrier, and retention of specific components in the ciliary membranes (Emmer et al., 2010; Garcia-Gonzalo and Reiter, 2012; Nachury et al., 2010). Disruption of these functions underlies a wide spectrum of disorders, known as ciliopathies, which are characterized by a variety of manifestations that include retinal degeneration, cystic kidneys, obesity and neural tube defects (Fliegauf et al., 2007; Gerdes et al., 2009; Sang et al., 2011; Valente et al., 2014).

A distinctive conversion of the rod photoreceptor primary cilium gives rise to the highly specialized light-sensing organelle known as the rod outer segment (ROS), which houses the light receptor rhodopsin and the associated phototransduction machinery. Despite the exceptionally high membrane influx that is necessary for the continuous replenishment of ROS membranes, their functional compartmentalization is maintained throughout the lifetime of the organism (Besharse et al., 2003; Pearring et al., 2013). Rhodopsin, the main constituent of the ROS membranes, is synthesized in the rod inner segment (RIS) and directly delivered to the periciliary location on rhodopsin transport carriers (RTCs) (Wang and Deretic, 2014). The nascent RTCs are formed at the Golgi and/or trans-Golgi network (TGN), where the activated small GTPase Arf4 recognizes and directly binds to the VxPx rhodopsin C-terminal targeting signal (Deretic et al., 2005). This leads to the assembly of a targeting complex containing Rab11a, the Arf GTPase-activating protein (GAP) ASAP1 and the Arf-Rab11 effector FIP3 (also known as RAB11FIP3) (Mazelova et al., 2009; Wang et al., 2012). The rhodopsin sequence encodes at least two ciliary targeting motifs, the VxPx and the FR, and they are conserved among other ciliary sensory receptors (Wang and Deretic, 2014; Wang et al., 2012). Notably, the VxPx motif enhances at least tenfold the ciliary targeting of a rhodopsin fusion protein in *Xenopus* rods, and accelerates the trafficking of post-Golgi vesicular structures, likely corresponding to RTCs (Lodowski et al., 2013). In addition, Arf4 reduction delays delivery of another ciliary sensory receptor, fibrocystin, from the Golgi complex to the cilium (Follit et al., 2014). Thus, the emerging physiological role of the VxPx motif and the Arf4-based ciliary targeting complex is to provide the directionality and increase the efficiency of ciliary receptor transport.

Recent insights into the molecular mechanisms of ciliary membrane targeting reveal high conservation of ciliary targeting motifs, as well as intracellular trafficking complexes that direct membrane delivery to this specific intracellular destination (Deretic, 2013; Follit et al., 2010; Follit et al., 2014; Geng et al., 2006; Jenkins et al., 2006; Knodler et al., 2010; Ward et al., 2011; Westlake et al., 2011). The Arf GAP ASAP1 has emerged as an essential scaffold protein that promotes communication between the Arf and Rab GTPases in ciliary trafficking, linking Arf4 to the Rab11–Rabin8–Rab8 ciliogenesis cascade (Deretic, 2013; Mazelova et al., 2009; Wang et al., 2012). ASAP1 acts as a

[1]Department of Surgery, Division of Ophthalmology, University of New Mexico, Albuquerque, NM 87131, USA. [2]Department of Cell Biology and Physiology, University of New Mexico, Albuquerque, NM 87131, USA.

*Author for correspondence (dderetic@salud.unm.edu)

**Received 5 September 2014; Accepted 3 February 2015**

Journal of Cell Science (2015) 128, 1375–1385 doi:10.1242/jcs.162925

coincidence detector for activated Arfs, acidic phospholipids and phosphatidylinositol 4,5-bisphosphate [PI(4,5)$P_2$], which regulates its GAP activity (Brown et al., 1998; Che et al., 2005). ASAP1 contains a BAR (Bin/amphiphysin/Rvs) domain (Peter et al., 2004), which mediates membrane tubulation and homodimerization, while also acting as an autoinhibitor of its GAP activity (Jian et al., 2009; Nie et al., 2006). Through its BAR domain, ASAP1 directly interacts with the Arf-Rab11 effector FIP3, which is a member of the distinct family of Rab11-interacting proteins that compete with each other for binding to Rab11, thus contributing to the diversity of Rab11 functions (Hales et al., 2001; Junutula et al., 2004; Prekeris et al., 2001). Binding of FIP3 to the BAR domain stimulates the Arf GAP activity of ASAP1 (Inoue et al., 2008). Therefore, the function of FIP3 in ciliary targeting might be to assist ASAP1 in the termination of the initial stage of RTC budding by controlling the timing of GTP hydrolysis on Arf4 (Wang and Deretic, 2014; Wang et al., 2012).

One of the essential roles of FIP3 is in abscission, the last step of cytokinesis that leads to the separation of two daughter cells (Fielding et al., 2005; Schiel et al., 2012; Wilson et al., 2005). During cytokinesis, Rab11 binding is necessary for FIP3 recruitment to recycling endosomes (Eathiraj et al., 2006). During interphase, FIP3 is involved in the maintenance of the recycling compartment (Horgan et al., 2007), along with ASAP1 (Inoue et al., 2008). The prominent roles of ASAP1, Rab11a and FIP3 in directing membrane flow out of the recycling endosomes to the cell surface, and from the TGN to the ciliary membrane, imply that molecular interactions between the Arf and Rab GTPases and their effectors in distinct trafficking pathways are well conserved. In this study, we show that FIP3 is an essential regulator of ciliary membrane targeting.

## RESULTS

### Rhodopsin is targeted to the primary cilia of kidney epithelial IMCD cells in a FIP3-dependent manner

The early synergistic interaction of rhodopsin with Arf4–GTP and ASAP1 leads to the recruitment of Rab11a and FIP3 to the Golgi and TGN (Mazelova et al., 2009; Wang et al., 2012). To define the precise role of FIP3 in ciliary targeting of rhodopsin, we expressed a fusion protein comprised of bovine rhodopsin followed by eGFP, followed by the repeat of eight C-terminal amino acids of rhodopsin containing the VxPx targeting signal (Rh–GFP–VxPx hereafter) in the mouse inner medullary collecting duct (IMCD) cells. We selected this model because epithelial IMCD3 and hTERT-RPE1 cells recapitulate the specific Arf4 and ASAP1-dependent ciliary localization of rhodopsin, including the transport of Rh–GFP–VxPx from the ciliary base to the tip using the conserved heterotrimeric kinesin-2 (Trivedi et al., 2012; Trivedi and Williams, 2010; Wang et al., 2012).

To determine whether FIP3 is an essential regulator of rhodopsin ciliary transport, IMCD3 cells expressing Rh–GFP–VxPx were transfected either with control non-targeting small interfering (si)RNA or with two different FIP3 siRNAs (Fig. 1). Control siRNA had no effect on ciliary targeting, in agreement with our previous study (Wang et al., 2012). Rh–GFP–VxPx (Fig. 1A, green) colocalized with acetylated tubulin present within the axoneme (Fig. 1A, red; arrows, yellow in merged images). Rh–GFP–VxPx was also detectable at the cilia tips, indicative of its transport along the ciliary membrane (Fig. 1A, XY, arrows in insets).

FIP3 siRNA#1 caused considerable changes in the localization of Rh–GFP–VxPx that included its periciliary accumulation (Fig. 1B, green, XY, arrows in insets; YZ, arrows on the right). Rh–GFP–VxPx was largely absent from the cilia detected with an antibody against acetylated tubulin (Fig. 1B, red, XZ, arrows; YZ, arrows on the left). In cells transfected with FIP3 siRNA#1, mislocalized Rh–GFP–VxPx was often diverted into membrane projections that developed in the close proximity to the cilia (Fig. 1B, XY arrows in insets; YZ, arrows on the right). FIP3 siRNA#2 had a similar effect on the localization of Rh–GFP–VxPx (Fig. 1C, green). Of the several cells transfected with FIP3 siRNA#2 seen at lower magnification, only one potentially localized Rh–GFP–VxPx to the cilium (Fig. 1C, arrow in the middle panel). Two boxed areas (magnified in the insets) show that FIP3 siRNA#2 interfered with the ciliary localization of Rh–GFP–VxPx, causing a complete absence of Rh–GFP–VxPx from the axoneme and the ciliary base (Fig. 1C, arrows in left insets) and substantial periciliary accumulation (Fig. 1C, arrows in right insets). Importantly, FIP3 siRNAs did not affect cilia length in IMCD3 cells (3.9±0.1 µm axoneme in control siRNA versus 3.8±0.1 µm and 3.7±0.3 µm in cells treated with FIP3 siRNA#1 and siRNA#2, respectively; $n=5$; ±s.e.m.).

Analysis of pixel colocalization by using Pearson's coefficient showed a negative correlation for Rh–GFP–VxPx and acetylated tubulin in cells treated with FIP3 siRNAs, which was significantly different from that found in controls ($P=9.75E^{-7}$ and $1.60E^{-6}$ for FIP3 siRNA#1 and #2, respectively) (Fig. 1D). Approximately 80% of the cells treated with control siRNA localized Rh–GFP–VxPx to primary cilia, but just a little over 20% of the cells transfected with FIP3 siRNA#1 properly targeted Rh–GFP–VxPx ($P=3.36E^{-4}$) (Fig. 1E). Treatment with siRNA#1 decreased FIP3 protein content to 20–40% of control levels (five separate experiments), while having negligible effect on the expression of ASAP1 (Fig. 1F). In experiments with FIP3 siRNA#2, <20% of the cells properly targeted Rh–GFP–VxPx, compared with >60% of the cells treated with control siRNA ($P=8.29E^{-4}$) (Fig. 1G). FIP3 protein content was decreased by siRNA#2 to ∼20% of control levels (three separate experiments), whereas this siRNA had minimal effect on the expression of Rab11 (Fig. 1H). By and large, in these experiments the phenotype of FIP3-depleted IMCD3 cells greatly resembled that of the ASAP1-depleted cells expressing Rh–GFP–VxPx (Wang et al., 2012), supporting the notion that FIP3 and ASAP1 function along the same ciliary pathway.

### Rhodopsin indirectly interacts with FIP3 through Rab11a and ASAP1 during its passage out of the photoreceptor Golgi and TGN

ASAP1, Arf4 and Rab11a directly interact with rhodopsin and FIP3 (Mazelova et al., 2009; Wang et al., 2012). To determine whether FIP3 and rhodopsin are in the same complex, we performed GST pulldowns from photoreceptor cell membranes with FIP3F1, the C-terminal end of FIP3, which stimulates RTC budding *in vitro* (Mazelova et al., 2009), or with FIP3C (Fig. 2A). GST–FIP3F1 (amino acids 441–756) encompassed the ASAP1, Arf4/5/6 and Rab11 binding sites (Inoue et al., 2008; Schonteich et al., 2007), whereas GST–FIP3C (amino acids 666–756) contained the Rab11 binding site.

To isolate photoreceptor biosynthetic membranes involved in rhodopsin trafficking, we fractionated retinal postnuclear supernatant (PNS) into Golgi/TGN-enriched fractions and RTCs, using an established methodology (Deretic and Mazelova, 2009).

Journal of Cell Science (2015) 128, 1375–1385 doi:10.1242/jcs.162925

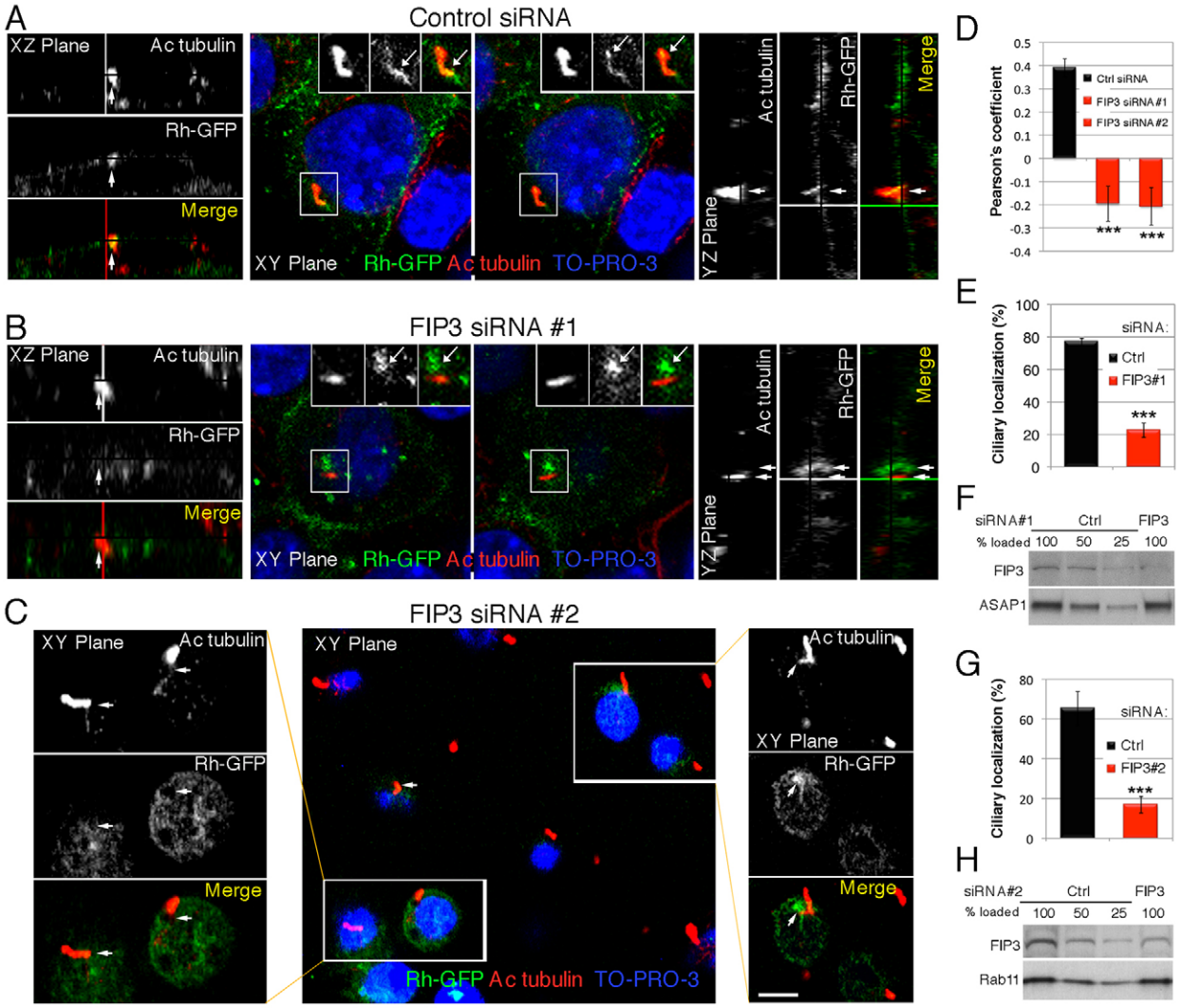


**Fig. 1. Rhodopsin is targeted to primary cilia of kidney epithelial IMCD3 cells in a FIP3-dependent manner.** (A) IMCD3 cells transiently expressing Rh–GFP–VxPx were transfected with control siRNA, fixed, stained with antibody against acetylated (Ac) tubulin and analyzed by confocal microscopy. Two consecutive confocal 0.9-µm sections are presented in the XY plane. Rh–GFP–VxPx (green) and acetylated tubulin (Cy3, red) colocalize in the ciliary axoneme (yellow). The boxed area is magnified and shown in separate channels in the insets. Rh–GFP–VxPx is detected at the proximal cilia and in the cilia tips (arrows in insets). (B) IMCD3 cells expressing Rh–GFP–VxPx (green) transfected with FIP3 siRNA#1. Two consecutive confocal 0.9-µm sections are presented in the XY plane. The boxed areas are magnified in the insets. Rh–GFP–VxPx (green, arrows) is localized around the cilium (red). In the YZ plane, a Rh–GFP–VxPx-filled membrane projection (green, right arrow) is juxtaposed to the cilium (red, left arrow). (C) The middle panel shows a field containing several cells expressing Rh–GFP–VxPx (green) transfected with FIP3 siRNA#2. The boxed areas are magnified in the insets. Rh–GFP–VxPx is absent from the cilia and the periciliary regions that appear as black holes (arrows in insets on the left). Rh–GFP–VxPx accumulates in the proximity of the ciliary base (arrows in insets on the right). Scale bar: 5 µm (A,B and insets in C), 3 µm (insets in A,B), 9 µm (C). (D) In a representative experiment, Rh–GFP–VxPx–acetylated-tubulin pixel colocalization analysis was performed within the cilia and expressed by the Pearson's coefficient ($n$=12 cells each for control and FIP3 siRNAs). Ctrl, control. Data show the mean±s.e.m.; ***$P$<0.0001). (E) Ciliary localization of Rh–GFP–VxPx in controls and cells treated with FIP3 siRNA#1 was determined in five separate experiments. The data were analyzed using Student's $t$-test ($n$=5, 4–10 cells in each experiment, a total of 32 cells for each condition) and are presented as the mean±s.e.m.; ***$P$=0.0003. (F) IMCD3 cells were lysed and proteins were separated by SDS-PAGE. Three different amounts of the siRNA control lysate were compared to the lysate from cells treated with FIP3 siRNA#1. The expression of FIP3 and ASAP1 in a representative experiment ($n$=5) was examined by immunoblotting. (G) Ciliary localization of Rh–GFP–VxPx in controls and cells treated with FIP3 siRNA#2 was determined in three separate experiments. The data were analyzed using Student's $t$-test ($n$=3, 4–6 cells in each experiment, a total of 22 cells for each condition) and are presented as the mean±s.e.m.; ***$P$=0.0008). (H) The expression of FIP3 and Rab11 in the cells treated with FIP3 siRNA#2 was examined by immunoblotting as above.

Arf4 was present nearly exclusively in the Golgi, whereas rhodopsin, ASAP1 and Rab11 were detected in the Golgi/TGN and on RTCs (Fig. 2B). We performed pulldowns from the Golgi/TGN preparation that was supplemented with the slowly hydrolysable GTP analog GppNHp to activate Arf4. GST–FIP3F1 pulled down rhodopsin, along with ASAP1 and Rab11, but the shorter GST–FIP3C performed even better in the pulldown (Fig. 2B). We reason that this reflected the ability of GST–FIP3C to incorporate – more readily than GST–FIP3F1 – into the endogenous ciliary targeting complex at the Golgi and TGN. Very little Arf4 was pulled down from the Golgi and TGN membranes, so we examined the ability of GST–FIP3F1 and GST–FIP3C to pull down Arf4 directly. Both GST–FIP3C and GST–FIP3F1 pulled down *Xenopus* and human Arf4 (Fig. 2C), although FIP3C

Journal of Cell Science (2015) 128, 1375–1385 doi:10.1242/jcs.162925

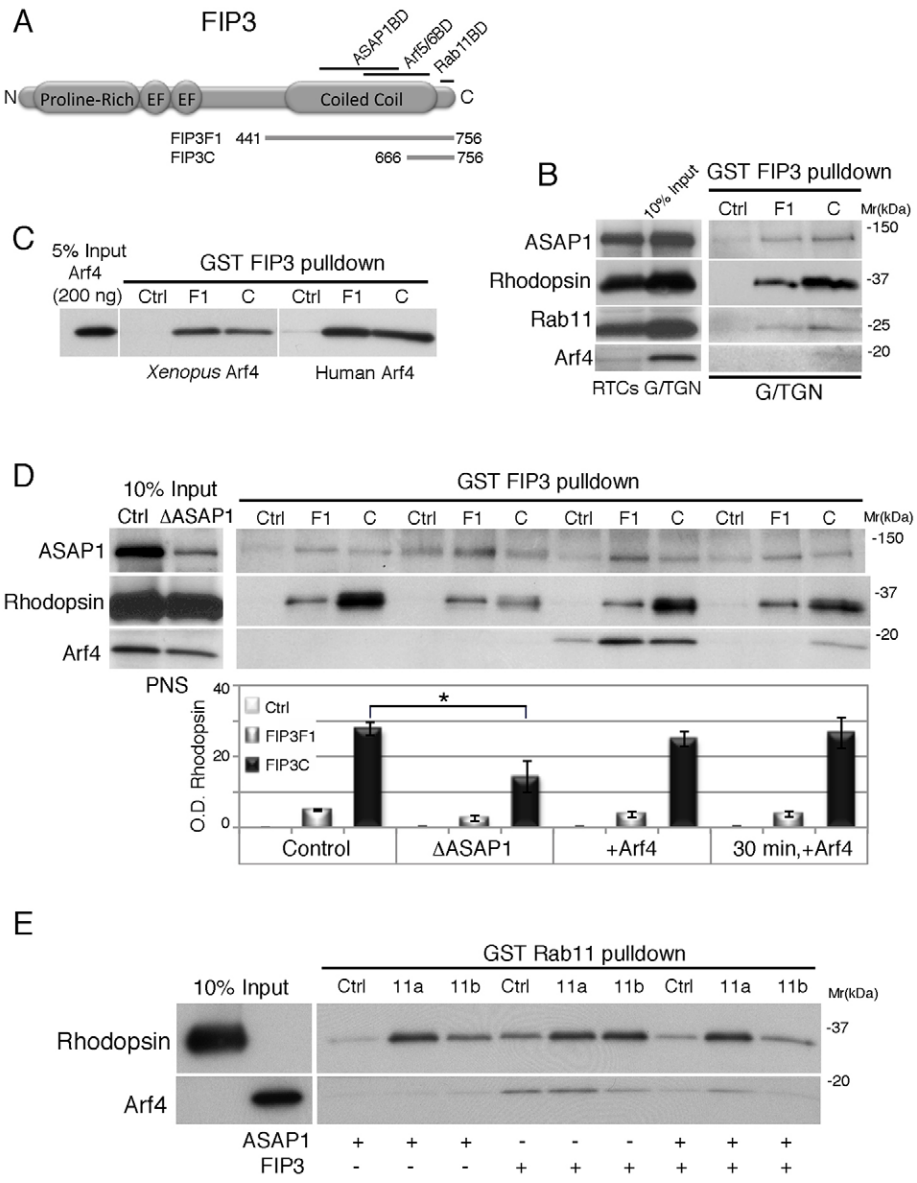


**Fig. 2. Rhodopsin interacts with FIP3 through ASAP1 and Rab11a during its passage out of the Golgi and TGN.** (A) The schematic structure of FIP3. ASAP1, Arf and Rab11 binding domains (BD) are indicated. (B) FIP3F1 (F1; amino acids 441–756) and FIP3C (C; amino acids 666–756) were expressed as GST fusion proteins and interacting retinal proteins were analyzed by immunoblotting, as indicated. G/TGN, Golgi and TGN; Ctrl, control. (C) GST–FIP3F1 and GST–FIP3C were incubated with either purified *Xenopus* or human Arf4, and bound Arf4 was detected by immunoblotting. (D) GST–FIP3F1 and GST–FIP3C were incubated either with the control or ASAP1-depleted frog retinal PNS. In some samples, recombinant Arf4–GppNHp was added to the control PNS, as indicated. Proteins were immunoblotted as indicated, and bound rhodopsin was quantified in three separate experiments. The data were analyzed using Student's *t*-test and are presented as the mean±s.e.m.; $*P=0.01$. (E) GST–Rab11a or GST–Rab11b were incubated with purified bovine rhodopsin, Arf4–GppNHp, ASAP1 (full length) and/or 6His–FIP3 (full length). Proteins bound to glutathione beads were analyzed by immunoblotting, as indicated.

contains only a portion of the Arf5/6 binding site (Inoue et al., 2008). This indicates that the Arf4 binding site on FIP3 is within amino acids 666–756, closer to the Rab11 binding site.

We sought to determine whether ASAP1, in addition to recruiting Rab11a (Wang et al., 2012), specifically recruits FIP3, thus allowing its indirect interaction with rhodopsin. Again, GST–FIP3C reproducibly pulled down six times more rhodopsin from the retinal PNS than GST–FIP3F1 (Fig. 2D). Immunodepletion of ASAP1 had little effect on the GST–FIP3F1 pulldown, but the access of GST–FIP3C to rhodopsin was significantly diminished ($P=0.01$) (Fig. 2D). Because FIP3C lacks the ASAP1 binding domain and contains the Rab11 binding domain, these data indicate that FIP3C indirectly pulls down rhodopsin by binding to endogenous Rab11, which is associated with ASAP1 and rhodopsin.

Because FIP3 is a known effector of activated Arf4, which directly binds to rhodopsin, we wanted to determine whether the addition of Arf4–GppNHp would increase the capacity of GST–FIP3F1 and GST–FIP3C to pull down rhodopsin. The addition of exogenous Arf4–GppNHp did not increase the ability of GST–FIP3F1 or GST–FIP3C to interact with rhodopsin, but increased their pulldown of Arf4 from the retinal PNS (Fig. 2D). However, when Arf4–GppNHp was added at 30 minutes following GST–FIP3F1 or GST–FIP3C, only a minimal amount of the exogenous Arf4 was pulled down (Fig. 2D). These data indicate that FIP3 recruits activated Arf4 concomitantly with incorporation into the ciliary targeting complex. When FIP3 is bound to the endogenous targeting complex, its interaction with exogenous activated Arf4 is greatly diminished.

To further examine the involvement of FIP3 in the ciliary targeting complex, we performed GST–Rab11a/b pulldown experiments using Arf4–GppNHp, purified rhodopsin, recombinant ASAP1 and/or 6His–FIP3 (Fig. 2E). Because FIP3 does not discriminate between Rab11a and Rab11b (Hales et al., 2001), both were able to precipitate rhodopsin and Arf4–GppNHp. A specific complex with rhodopsin was formed when Arf4–GppNHp, ASAP1 and Rab11a were present (Fig. 2E), as determined in previous studies (Wang et al., 2012). When FIP3

Journal of Cell Science (2015) 128, 1375–1385 doi:10.1242/jcs.162925

and ASAP1 were added together, both the specificity of interaction with Rab11a and the recruitment of Arf4–GppNHp were increased compared to those observed with FIP3 and ASAP1 individual pulldowns (Fig. 2E), indicating their cooperative function in the assembly of the rhodopsin-targeting complex.

### ASAP1 binds rhodopsin and FIP3 in a mutually exclusive manner

The binding site for both rhodopsin and FIP3 has been mapped to the ASAP1 BAR domain (Inoue et al., 2008; Mazelova et al., 2009); therefore, we wanted to establish whether rhodopsin and FIP3 compete for binding to ASAP1. To test this, we examined the simultaneous binding of purified rhodopsin and FIP3F1 to 6His–BAR-PZA, a recombinant protein composed of the BAR, PH, GAP and ankyrin repeat domain of ASAP1 (Fig. 3A). We chose 6His–BAR-PZA because it stimulates RTC budding *in vitro* and is more efficient in rhodopsin–Arf4–GTP pulldowns than the full-length ASAP1 (Mazelova et al., 2009; Wang et al., 2012). FIP3F1 substantially competed the binding of 60 nM rhodopsin to BAR-PZA (Fig. 3B). Similarly, rhodopsin competed the binding of 15 nM FIP3F1 to BAR-PZA (Fig. 3B), suggesting that the binding sites for rhodopsin and FIP3 on the ASAP1 BAR domain are at least partially overlapping. FIP3F1 displaced rhodopsin from the ternary complex with BAR-PZA and Arf4–GTP, but had a negligible effect on the association of BAR-PZA with Arf4–GTP within this complex (Fig. 3C,D). Collectively, these data indicate that the Arf4–GTP-bound ASAP1 can form a complex either with rhodopsin or with FIP3, and that a dynamic equilibrium between these complexes likely controls GTP hydrolysis on Arf4 by ASAP1, and the exit of rhodopsin from the Golgi and TGN.

### Rhodopsin is in close proximity to FIP3 at the Golgi and TGN but not on RTCs

To corroborate our binding experiments, we examined FIP3 interactions with rhodopsin and the ciliary targeting complex in photoreceptors, using the established *in situ* proximity ligation assay (PLA), which we modified previously for the analysis of vertebrate retinas (Wang et al., 2012). Briefly, PLA is based on the dual recognition of a target protein complex by two primary antibodies and two secondary antibodies covalently attached to unique oligonucleotides that – through a series of enzymatic reactions and hybridization with fluorescently labeled oligonucleotide probes – generate a binary output in the form of ~0.5 µm dots, which are

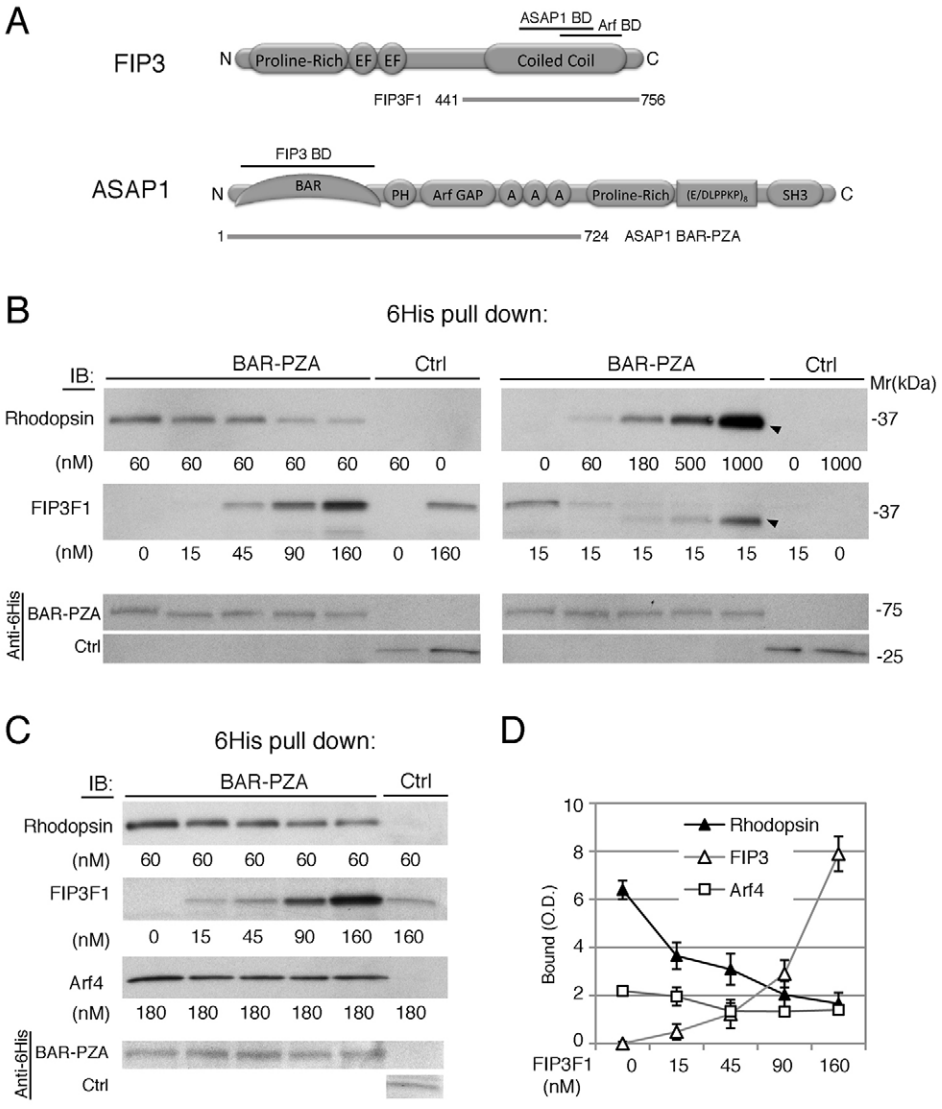


**Fig. 3. ASAP1 binds to rhodopsin and FIP3 in a mutually exclusive manner.** (A) Schematic structures of FIP3 and ASAP1. Mutual binding domains (BD) are indicated. (B) Recombinant 6His–BAR-PZA was incubated with purified bovine rhodopsin followed by increasing concentrations of GST–FIP3F1, or vice versa. Proteins bound to Ni-NTA–agarose beads were immunoblotted (IB) as indicated. Ctrl, control. (C) Recombinant 6His–BAR-PZA was incubated with purified bovine rhodopsin and Arf4–GppNHp, followed by increasing concentrations of GST–FIP3F1. (D) Bound rhodopsin, FIP3 and Arf4 were quantified in three separate experiments. Data show the mean±s.e.m..

Journal of Cell Science (2015) 128, 1375–1385 doi:10.1242/jcs.162925

visualized by microscopy (Söderberg et al., 2006; Trifilieff et al., 2011). Because the positive signal is possible only when the PLA probes are in close proximity (<40 nm), the maximal detected distance is within the limits of protein–protein interactions, so PLA is well suited for the detection of stable and transient interactions *in situ* at endogenous protein levels. PLA is particularly appropriate for the analysis of interactions within the ciliary targeting complex in vertebrate photoreceptors, because of the extraordinarily high unidirectional ciliary membrane flow within these exquisitely polarized cells that are well-aligned and organized in a single retinal layer, which is readily identified by differential interference contrast (DIC) microscopy, nuclear staining and specific organelle markers (Blasic et al., 2012; Wang et al., 2012).

Using previously characterized specific antibodies (Mazelova et al., 2009; Wang et al., 2012), we detected rhodopsin–FIP3 interactions by PLA almost exclusively in the Golgi area (Fig. 4A, red dots) in the photoreceptor myoid region (M; see the schematic of the photoreceptor cell, Fig. 4G). Rhodopsin–FIP3 interactions were abolished by treatment with cycloheximide (Fig. 4B,C), which clears rhodopsin from the biosynthetic membranes and the Golgi (Fig. 4A,B, arrows in insets). Thus, FIP3 specifically interacts with newly synthesized rhodopsin at the exit from the Golgi and TGN. Whereas rhodopsin–FIP3 interaction sites were highly concentrated only at the Golgi and TGN (Fig. 4D), ASAP1 and Rab11 also colocalized with FIP3 on RTCs, in the ellipsoid region (E; Fig. 4E,F, arrows). Rhodopsin–ASAP1 interaction sites were distributed between the Golgi, TGN and RTCs, as previously reported (Wang et al., 2012) (Fig. 4H). PLA quantification, using an established methodology (Wang et al., 2012), which is also detailed in Fig. 4H, showed that ~90% of the rhodopsin–FIP3 interaction sites are at the Golgi and TGN, whereas only ~10% are on RTCs (Fig. 4I). Thus, rhodopsin is in the vicinity of FIP3 nearly exclusively at the Golgi and TGN, whereas FIP3 interactions with ASAP1 and Rab11 persist on RTCs, where close to 30% of interaction sites are localized. The equal proportion of interaction sites containing ASAP1+rhodopsin or ASAP1+FIP3 on RTCs

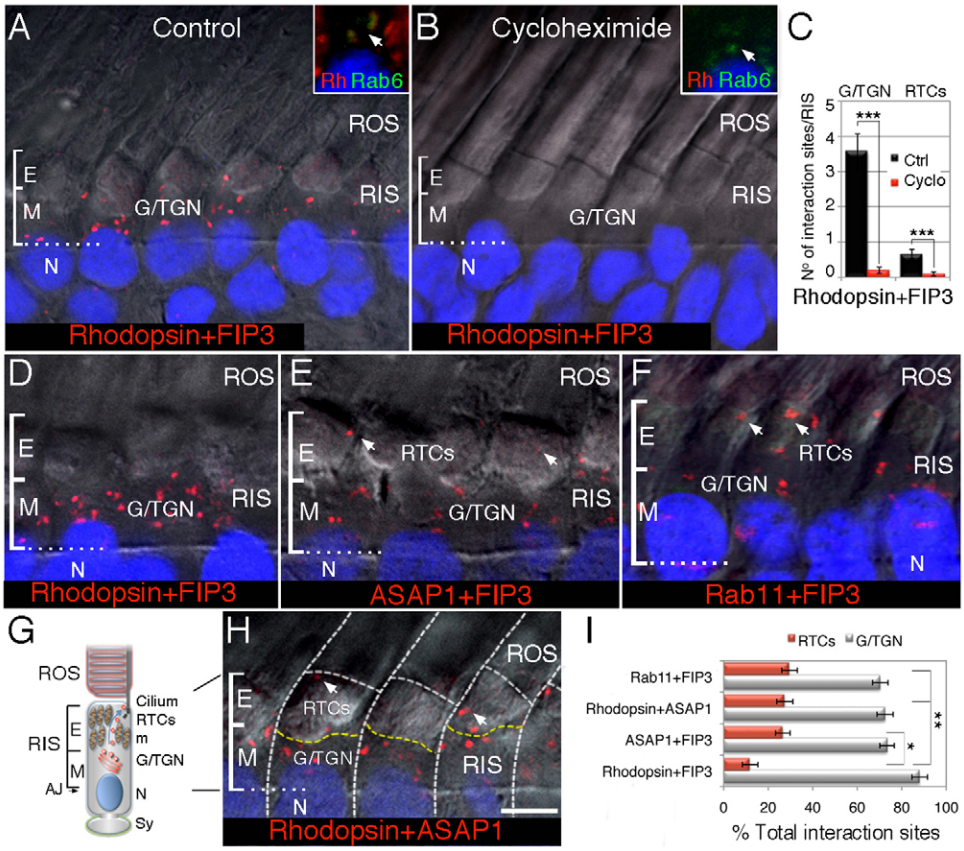


**Fig. 4. FIP3 is in proximity to rhodopsin predominantly at the Golgi and TGN.** (A) Rhodopsin–FIP3 interaction sites (red dots) were detected by PLA in control retinas. Retinal sections were visualized by DIC. The dotted line indicates the outer limiting membrane (OLM, comprised of adherens junctions). Nuclei (N) were stained with TO-PRO-3 (blue). (B) No rhodopsin–FIP3 interaction sites are detected in retinas in which protein synthesis is inhibited by cycloheximide. Insets in A and B show retinas that were double-labeled with anti-rhodopsin mAb 11D5 (red) and anti-Rab6 (green), a trans-Golgi marker. (C) Red fluorescent signals (dots) were quantified in control (Ctrl) and cycloheximide (Cyclo)-treated retinas. The data from a representative experiment ($n=3$) were analyzed using Student's *t*-test ($n=30$) and are presented as the mean±s.e.m.; ***$P<0.0001$. (D) Rhodopsin–FIP3 interaction sites (red dots) were detected by PLA. The same experiment was repeated for (E) ASAP1–FIP3 and (F) Rab11–FIP3. Arrows indicate interaction sites on RTCs. (G) Diagram of a photoreceptor cell. Primary cilium elaborates the ROS. The Golgi and the TGN (G/TGN) are localized in the myoid region (M) of the RIS. RTCs that bud from the TGN are targeted to the cilium (arrow), through the ellipsoid region ('E') filled with mitochondria (m). AJ, adherens junctions; N, nucleus; Sy, synapse. (H) Rhodopsin–ASAP1 PLA. The quantification methodology is summarized in this panel. White dashed lines outline individual photoreceptors and the RIS/ROS border. Yellow dashed lines demarcate the border of the ellipsoid and myoid regions of the RIS, which is detectable in the DIC image. Red dots within the myoid were counted as the Golgi or TGN interaction sites, whereas those in the ellipsoid were counted as RTC interaction sites. Scale bars: 7 µm (A,B), 5 µm (D–F,H and insets in A,B). (I) Red fluorescent signals (dots) were counted and the data from a representative experiment ($n=3$) were expressed as a percentage of total interaction sites within the RIS, analyzed using Student's *t*-test ($n=62$) and presented as the mean±s.e.m.; **$P<0.001$, *$P<0.01$.

Journal of Cell Science (2015) 128, 1375–1385 doi:10.1242/jcs.162925

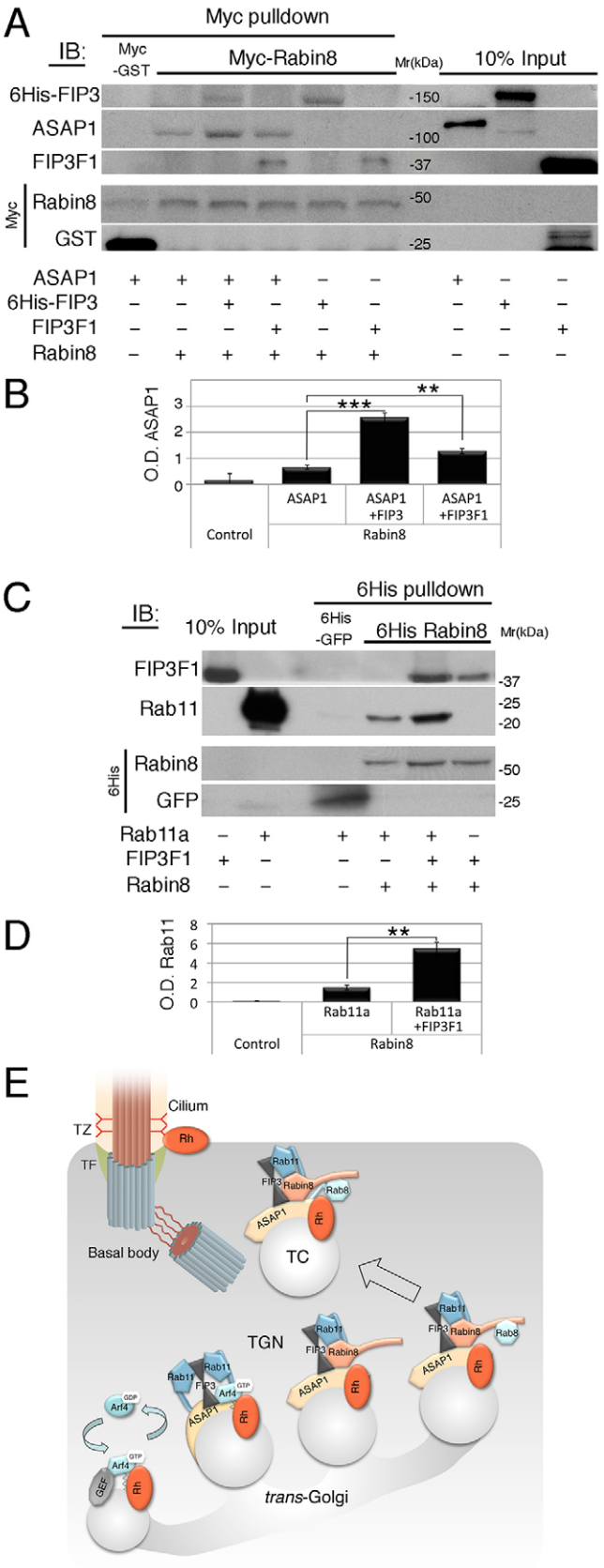


**Fig. 5. FIP3 increases the interactions of ASAP1 and Rab11a with the Rab8 GEF Rabin8.** (A) Myc–Rabin8 bound to anti-Myc beads, or Myc–GST as a control, were incubated with recombinant ASAP1, with or without 6His–FIP3 or untagged FIP3F1. Bound proteins were detected by immunoblotting (IB), as indicated. (B) ASAP1 bound to anti-Myc beads was quantified in five separate experiments. Data are presented as the mean±s.e.m.; ***$P<0.0001$, **$P=0.005$. (C) 6His–Rabin8, or 6His–GFP as a control, were incubated with recombinant Rab11a, with or without FIP3F1. Proteins bound to Ni-NTA–agarose beads were detected by immunoblotting, as indicated. (D) Rab11a was quantified in three separate experiments. Data are presented as the mean±s.e.m.; **$P<0.005$. (E) A diagram summarizing the sequence of molecular interactions likely taking place en route to cilia. Our study suggests that FIP3 constrains the binding site for Rabin8 within the ASAP1–Rab11a–FIP3 targeting complex at the Golgi and TGN, likely optimizing the positioning of the extended Rabin8 GEF domain for the subsequent activation of Rab8 on transport carriers (TC). Rh, rhodopsin; TZ, transition zone; TF, transition fiber.

suggests that ASAP1 partitions between two complexes: one with rhodopsin and the other with FIP3. Alternatively, a single large complex on RTCs might contain rhodopsin and FIP3, but their placement might be outside the range of detection by PLA.

### FIP3 shapes the binding pocket for Rabin8 within the ASAP1–Rab11a–FIP3 targeting complex

During RTC budding, ASAP1 acts as a scaffold that recruits to RTCs Rab8–GDP and its guanine nucleotide exchange factor (GEF) Rabin8 (Wang et al., 2012), both of which are essential regulators of fusion with the plasma membrane and ciliogenesis (Feng et al., 2012; Hattula et al., 2002; Knodler et al., 2010; Moritz et al., 2001; Nachury et al., 2007; Westlake et al., 2011). Because Rabin8 functions downstream of FIP3, we wanted to determine whether in ciliary trafficking Rabin8 cooperates with, or displaces FIP3 from ASAP1. We performed Myc–Rabin8 pulldowns of ASAP1, with or without the prebound 6His–FIP3 or FIP3F1. 6His–FIP3 significantly increased ASAP1–Rabin8 interaction ($P=2.85E^{-3}$; Fig. 5A,B). FIP3F1 had a similar but smaller effect ($P=0.016$). Moreover, in the absence of ASAP1, Myc–Rabin8 pulled down 6His–FIP3 and FIP3F1 (Fig. 5A), suggesting that FIP3 and ASAP1 bind separately to Rabin8. Because FIP3 is an effector of Rab11, we next wanted to examine the association between Rabin8, FIP3 and Rab11a. We performed 6His–Rabin8 pulldowns of Rab11a, with or without the prebound FIP3F1. We chose FIP3F1 because it functions as an effector of Rab11 that stimulates RTC budding *in vitro* (Mazelova et al., 2009). FIP3F1 significantly increased Rab11a–Rabin8 interaction ($P=5.65E^{-3}$; Fig. 5C,D). 6His–Rabin8 also pulled down FIP3F1 in the absence of Rab11a (Fig. 5C), suggesting that FIP3 and Rab11a bind separately to Rabin8. We have previously established that ASAP1 and Rab11a bind independently to Rabin8 (Wang et al., 2012). Thus, the FIP3-mediated threefold increase in Rabin8 binding to both ASAP1 and Rab11 suggests that FIP3 shapes the Rabin8 binding site formed by Rab11 and ASAP1 within the ciliary targeting complex. Our data support the notion that by enhancing the recruitment of Rabin8, FIP3 imparts additional stringency to the spatiotemporally restricted Rab8 activation in ciliary transport. Fig. 5E schematically represents the sequence of molecular interactions within the ASAP1–Rab11–FIP3–Rabin8 complex that regulates ciliary receptor targeting, consistent with the results of our study.

## DISCUSSION

In this study, we show that FIP3 is an essential regulator of ciliary trafficking. We demonstrate that FIP3 controls rhodopsin–ASAP1 interactions and displaces rhodopsin from the ternary complex

Journal of Cell Science (2015) 128, 1375–1385 doi:10.1242/jcs.162925

with Arf4–GTP and ASAP1, a property that likely links rhodopsin incorporation into RTCs with GTP hydrolysis on Arf4 by ASAP1. Furthermore, we show that FIP3 increases the interactions of Rab11a and ASAP1 with their downstream partner, the Rab8 GEF Rabin8, which accordingly acts as a coincidence detector for progression to the next step in ciliary targeting. Therefore, FIP3 is a crucial component that assists ASAP1 and Rab11a in the stepwise assembly of the ciliary targeting complex, which regulates the ordered succession of small GTPases that direct cargo progression to the cilia.

The regulatory role of FIP3 in ciliary trafficking is associated with its ability to interact with ASAP1, which functions as a GAP and an effector of Arf4 (Mazelova et al., 2009). Conformational changes in ASAP1, induced by FIP3 and PI(4,5)$P_2$ binding, regulate the GAP activity of ASAP1 (Che et al., 2005; Inoue et al., 2008; Jian et al., 2009). Thus, FIP3 might assist ASAP1 in terminating the first, Arf4-dependent stage of the assembly of the rhodopsin ciliary targeting complex (Wang and Deretic, 2014). PI(4,5)$P_2$ and phosphoinositide-binding proteins cooperate with Rab8 in preparation for RTC fusion to the target RIS plasma membrane (Deretic et al., 2004). However, PI(4,5)$P_2$ inhibits ASAP1–FIP3 interactions (Inoue et al., 2008). As the PI(4,5)$P_2$ content appears to increase as RTCs reach the fusion site, this might gradually diminish ASAP1–FIP3 interaction en route to cilia. Consequently, the regulation of PI(4,5)$P_2$ levels might control not only ASAP1 GAP activity, but also its FIP3-assisted functional transition during RTC maturation – from the termination of RTC budding, to Rabin8 recruitment and Rab8 activation in preparation for RTC fusion.

The depletion of FIP3 from IMCD3 cells produces a phenotype that closely resembles the depletion of ASAP1, which causes the formation of the actin-based protrusions in proximity to primary cilia (Wang et al., 2012), in keeping with its important role in cytoskeleton dynamics (Randazzo et al., 2000). FIP3 is involved in the regulation of the actin cytoskeleton both in late telophase, which is essential for the severing of the connecting bridge between daughter cells during cytokinesis (Schiel et al., 2012), and in breast cancer cell migration (Jing et al., 2009). Because blocking actin assembly facilitates ciliogenesis (Kim et al., 2010), the role of FIP3 and ASAP1 might include the control of actin polymerization in the periciliary region to facilitate ciliary trafficking.

Activated Arf4 significantly increases direct ASAP1–rhodopsin interaction (Wang et al., 2012). Our current study shows that FIP3 significantly increases direct ASAP1–Rabin8 interaction. Collectively, our data indicate that the sequential interactions with ASAP1 control cargo progression and the direction of ciliary traffic. GTP hydrolysis on Arf4 terminates the early rhodopsin–Arf4–ASAP1 complex at the Golgi and TGN. Phosphorylation of Rabin8 might modulate its interactions with ASAP1 and Rab11a as they progress towards the cilia. Rabin8 is recruited to the membrane by specific phospholipids and a serine/threonine kinase NDR2 (also called STK38L) (Chiba et al., 2013). Recently, NDR2 was identified as a canine retinal degeneration gene, mutations in which result in a condition corresponding to the human ciliopathy Leber congenital amaurosis (LCA), which is characterized by severe loss of visual function (Berta et al., 2011; Goldstein et al., 2010). Thus, the precise regulation of Rabin8 during ciliary trafficking in vertebrate photoreceptors has powerful influence on their homeostasis.

Rab11–FIP3 interactions are important in all FIP3 functions (Eathiraj et al., 2006; Mazelova et al., 2009; Wilson et al., 2005). Rab11 has been implicated in the regulation of plasma membrane trafficking through the recycling endosomes (Prekeris et al., 2000) or through the TGN, where it is recruited by phosphatidylinositol 4-kinase β (PI4Kβ) (de Graaf et al., 2004). A recent study has shown that PI4Kβ can simultaneously recruit the Rab11–GTP–FIP3 complex or Rab11–GDP (Burke et al., 2014). A ternary complex can be formed between Rab11–GTP, FIP3 and ASAP1 (Inoue et al., 2008). We observed that, like PI4Kβ, ASAP1 also recruits Rab11–GTP–FIP3 or Rab11–GDP (Mazelova et al., 2009; Wang et al., 2012). We hypothesize that, at the TGN, Rab11–GDP could be activated by a yet-to-be-identified vertebrate GEF, resulting in the formation of the ASAP1–Rab11–GTP–FIP3 complex. Rab11–GTP interacts both with FIP3 and Rabin8 (Eathiraj et al., 2006; Knodler et al., 2010). Our study shows that these interactions are not mutually exclusive. On the contrary, the ASAP1–Rab11a–GTP–FIP3 complex has a greater affinity for Rabin8, compared to individual affinities, indicative of their cooperative function in Rabin8 recruitment and Rab8 activation in ciliary trafficking.

FIP3 is also a known Arf effector (Hickson et al., 2003; Schonteich et al., 2007; Shin et al., 1999). Thus, our finding that activated Arf4 did not increase rhodopsin–FIP3 interactions was surprising. It suggests that activated Arf4 is not responsible for the recruitment of FIP3 into the ciliary targeting complex. FIP3 is required for Arf6 recruitment to the midbody during late telophase (Schonteich et al., 2007). Our data suggest that FIP3 might be involved in recruiting and positioning activated Arf4 into the ciliary targeting complex, likely to support recurring carrier biogenesis. However, the diminished ability to recruit additional activated Arf4 when FIP3 is a part of the complex might be important to impart directionality to ciliary transport.

Both rhodopsin and FIP3 bind to the BAR domain of ASAP1 (Inoue et al., 2008; Mazelova et al., 2009). Rhodopsin binding to ASAP1 possibly allows its packaging into RTCs by blocking GTP hydrolysis on Arf4. Displacement of rhodopsin from ASAP1 by FIP3 might couple GTP hydrolysis on Arf4 with rhodopsin packaging into RTCs. FIP3 binding, which causes an activating change in ASAP1 (Inoue et al., 2008), also exposes its Rabin8 binding site, so we conclude that Rabin8 binds to the catalytically active ASAP1 in complex with Rab11a and FIP3. Rabin8 preference for the active conformation of ASAP1 might prevent its premature inclusion into the ciliary targeting complex, as Rabin8 is necessary for the later post-Arf4 stage of RTC budding (Wang and Deretic, 2014). Rabin8-mediated activation of Rab8 renders RTCs competent for fusion with the periciliary plasma membrane, because activated Rab8 regulates the final stages of polarized membrane traffic, fusion of ciliary-targeted carriers and ciliogenesis (Deretic et al., 1995; Knodler et al., 2010; Moritz et al., 2001; Nachury et al., 2007; Wang et al., 2012; Yoshimura et al., 2007).

In summary, we show that FIP3 acts synergistically with ASAP1 and Rab11a to couple the successive activation of Arf and Rab GTPases with the forward movement of ciliary cargo. Because FIP3 and ASAP1 act as homodimers (Eathiraj et al., 2006; Nie et al., 2006), the complexes they form together might comprise a protein coat that regulates TGN-to-cilia trafficking. Future investigation should provide invaluable information about the architecture and function of this putative coat. Nevertheless, the data presented here implicate FIP3 as an indispensable regulator of ciliary membrane expansion and compartmentalization of signaling receptors, with potential involvement in ciliopathies and other human diseases.

## MATERIALS AND METHODS

### Materials

Mammalian expression vector encoding bovine rhodopsin–eGFP was a kind gift of David Williams (University of California, Los Angeles, CA).

Purified bovine rhodopsin was a gift of Kris Palczewski (Case Western Reserve University, OH). The primary antibodies used in this study were as follows: rabbit polyclonal anti-Arf4 (Mazelova et al., 2009); anti-rhodopsin C-terminus monoclonal antibody (mAb) 11D5 (Deretic and Papermaster, 1991); monoclonal anti-ASAP1, anti-Rab8 and anti-Rab11 (BD Biosciences); rabbit polyclonal anti-ASAP1 (Randazzo et al., 2000); rabbit polyclonal anti-Rab6 and goat polyclonal anti-Rab11 (Santa Cruz Biotechnology); mouse anti-acetylated tubulin (Sigma); goat anti-GST (Amersham Biosciences); rabbit anti-6His (Novus Biologicals); and mouse anti-6His (Qiagen). Rabbit polyclonal anti-Rabin8 (Hattula et al., 2002) and Myc–Rabin8 were gifts of Johan Peranen (University of Helsinki, Finland). Goat and rabbit polyclonal anti-FIP3, GST–FIP3, GST–FIP3F1, GST–Rab11a, GST–Rab11b, in the pGEX-KG vector, were kind gifts of Rytis Prekeris (University of Colorado, CO). 6His–BAR-PZA, 6His–ASAP1 and rabbit polyclonal anti-ASAP1 were kind gifts of Paul Randazzo (NCI/NIH). Duolink II Rabbit/Mouse Red Kit (excitation, 598 nm; emission, 634 nm) was from Olink Bioscience.

### Double transfection of rhodopsin–GFP–VxPx and FIP3 siRNA

FIP3 siRNA oligonucleotides were obtained from Thermo Scientific Dharmacon. The target sequence for siRNA#1 was 5′-GGGCAAUGA-GGCAGAACUA-3′, and for siRNA#2 5′-GGUCAUCUUCCUAGAG-AGAUU-3′. siGENOME non-targeting siRNA#3 from Thermo Scientific Dharmacon was used as a control. Mouse IMCD-3 cells obtained from ATCC were plated on T75 Falcon culture flasks in DMEM/F12 medium (ATCC) with 10% fetal bovine serum (GIBCO). Cells were trypsinized and transferred to six-well culture plates (Costar) in pre-warmed medium and incubated at 37℃ and 5% $CO_2$ for 24 hours to 50% confluence. Transfection of FIP3 siRNA was performed following the manufacturer's protocol (Lipofectamine RNAiMAX). Briefly, 60 pmol of FIP3 siRNA was added to 0.25 ml of the reduced-serum medium OPTI-MEM (GIBCO). Lipofectamine RNAiMAX (6 µl) was diluted in 0.25 ml of OPTI-MEM. Diluted siRNA duplexes and diluted Lipofectamine RNAiMAX were combined and incubated for 20 minutes at room temperature. This complex was added to cells and incubated for 5 hours. Cells were then transiently transfected with a pcDNATM3.1 mammalian expression vector encoding bovine rhodopsin followed by eGFP followed by the repeat of eight C-terminal amino acids of rhodopsin (rhodopsin–GFP–VxPx). Transfection was performed with Lipofectamine LTX and PLUS Reagents (Invitrogen) following the manufacturer's protocol. Briefly, 2 µg of plasmid and 2 µl of PLUS reagent were added to 0.25 ml of OPTI-MEM and incubated at room temperature for 5 minutes. Lipofectamine LTX (10 µl) was diluted in 0.25 ml of OPTI-MEM. Plasmid and Lipofectamine LTX solutions were mixed and incubated for 30 minutes at room temperature. This complex was added to cells and incubated overnight, before changing to DMEM/F12 medium with 10% FBS. After 4 hours, medium was replaced with serum starvation medium (0.5% serum in DMEM/F12 medium) and the cells were incubated for an additional 18–20 hours. The efficiency of protein depletion was assessed by western blotting. The transfection efficiency of rhodopsin–GFP–VxPx was examined by confocal microscopy. Confocal optical sections were generated on a Zeiss 510 Laser Scanning Confocal Microscope (Carl Zeiss, Inc.), mounted on an Axioplan 2 upright microscope, using a 40× Achroplan objective and a 488-nm argon ion laser, and 543-nm and 633-nm HeNe lasers. Digital images were prepared using Adobe Photoshop CS (Adobe Systems Inc.).

### GST fusion protein pull-down assay

Purified GST fusion proteins or GST alone (5 µg each) were incubated with frog retinal fractions in 500 µl of reaction buffer (50 mM HEPES pH 7.4, 150 mM NaCl, 5 mM $MgCl_2$•$6H_2O$, 0.1% Triton X-100 and 0.1% BSA) in the presence or absence of 5 µg *Xenopus* Arf4 with 100 µM GppNHp at 37℃ for 30 minutes, followed by 1 hour at 4℃. GST fusion proteins were immobilized on glutathione–Sepharose-4B beads (30 µl per sample) by incubation at 4℃ for 1 hour, and the beads were washed six times with reaction buffer. Bound proteins were eluted in 20 µl of 2× SDS-PAGE sample buffer and analyzed by SDS-PAGE and western blotting.

### His-tag protein pulldown assay

The purified His-tagged proteins (5 µg each) 6His–BAR-PZA and TAT–6His–GFP (used as a control) were immobilized on Ni-NTA–agarose beads (30 µl per sample with 200 µl PBS) by incubation at 4℃ for 1 hour and washed once with PBS containing 15 mM imidazole. Immobilized His-tagged proteins were then incubated either with a fixed amount of purified bovine rhodopsin and different amounts of recombinant FIP3-F1 or with a fixed amount of FIP3-F1 and different amounts of rhodopsin in the presence of 20 µM GppNHp in 500 µl of reaction buffer at room temperature for 2 hours. 6His–Rabin8 and TAT–6His–GFP were also incubated with Rab11a in the presence or absence of FIP3F1 for 2 hours at 4℃. Following incubations, Ni-NTA–agarose beads were washed six times with reaction buffer containing 15 mM imidazole. Bound proteins were eluted in 20 µl of 2× SDS-PAGE sample buffer and analyzed as above.

### Myc fusion protein pulldown assay

Myc–Rabin8 was immobilized on anti-Myc–agarose beads by incubating Myc–Rabin8 cell lysate (from a 250-ml culture) with anti-Myc–agarose beads (250 µl) at 4℃ overnight, followed by ten washes with PBS. ASAP1 and 6His–FIP3, or FIP31, were added to Myc–Rabin8 immobilized on the anti-Myc–agarose beads (30 µl per sample) and incubated in reaction buffer, as above, at 4℃ for 3 hours. Anti-Myc–agarose beads were then washed six times with reaction buffer. Bound proteins were eluted in 20 µl of 2× SDS-PAGE sample buffer and analyzed as above.

### Proximity ligation assay

Confocal microscopy was performed on dark-adapted frog retinas. Isolated eyecups were fixed with 4% paraformaldehyde overnight and embedded in 5% agarose. In some experiments, eyecups were first incubated for 5 hours with or without 25 µg/ml cycloheximide. Sections (100 µm) were cut and permeabilized in 0.1% Triton X-100. The fluorescence assay was performed using Duolink II Rabbit/Mouse Red Kit (Olink Bioscience #92101) following the manufacturer's protocol, with modification for brain slices (Trifilieff et al., 2011) as described previously (Wang et al., 2012). Frog retinal sections were incubated in blocking solution provided by the manufacturer for 1 hour at room temperature. Only previously validated antibodies were used for these experiments. Sections were incubated with two primary antibodies overnight at 4℃. Two PLA probes were applied to the samples and incubated overnight at 4℃. Ligases in ligation solution were added to samples and incubated for 1 hour at 37℃, followed by the Amplification-Polymerase solution for 200 minutes at 37℃. Sections were counterstained with the nuclear stain TO-PRO-3 and examined by confocal microscopy.

#### Acknowledgements

We thank Drs Kris Palczewski, Johan Peranen, Rytis Prekeris, Paul Randazzo and David Williams for their generous gifts of reagents.

#### Competing interests

The authors declare no competing or financial interests.

#### Author contributions

Both authors planned the experiments and wrote the methods. J.W. perfomed all experiments. D.D. performed the quantitative analysis and wrote the manuscript.

#### Funding

This work was supported by the National Institutes of Health [grant number EY-12421]. UNM Fluorescence Microscopy Facility is supported by National Center for Research Resources, National Science Foundation, National Cancer Institute and the UNM Cancer Center. Deposited in PMC for release after 12 months.

#### References

**Berta, A. I., Boesze-Battaglia, K., Genini, S., Goldstein, O., O'Brien, P. J., Szél, Á., Acland, G. M., Beltran, W. A. and Aguirre, G. D.** (2011). Photoreceptor cell death, proliferation and formation of hybrid rod/S-cone photoreceptors in the degenerating STK38L mutant retina. *PLoS ONE* **6**, e24074.

**Besharse, J. C., Baker, S. A., Luby-Phelps, K. and Pazour, G. J.** (2003). Photoreceptor intersegmental transport and retinal degeneration: a conserved pathway common to motile and sensory cilia. *Adv. Exp. Med. Biol.* **533**, 157-164.

**Blasic, J. R., Jr, Lane Brown, R. and Robinson, P. R.** (2012). Light-dependent phosphorylation of the carboxy tail of mouse melanopsin. *Cell. Mol. Life Sci.* **69**, 1551-1562.

**Brown, M. T., Andrade, J., Radhakrishna, H., Donaldson, J. G., Cooper, J. A. and Randazzo, P. A.** (1998). ASAP1, a phospholipid-dependent arf GTPase-activating protein that associates with and is phosphorylated by Src. *Mol. Cell. Biol.* **18**, 7038-7051.

**Burke, J. E., Inglis, A. J., Perisic, O., Masson, G. R., McLaughlin, S. H., Rutaganira, F., Shokat, K. M. and Williams, R. L.** (2014). Structures of PI4KIIIβ complexes show simultaneous recruitment of Rab11 and its effectors. *Science* **344**, 1035-1038.

**Che, M. M., Boja, E. S., Yoon, H. Y., Gruschus, J., Jaffe, H., Stauffer, S., Schuck, P., Fales, H. M. and Randazzo, P. A.** (2005). Regulation of ASAP1 by phospholipids is dependent on the interface between the PH and Arf GAP domains. *Cell. Signal.* **17**, 1276-1288.

**Chiba, S., Amagai, Y., Homma, Y., Fukuda, M. and Mizuno, K.** (2013). NDR2-mediated Rabin8 phosphorylation is crucial for ciliogenesis by switching binding specificity from phosphatidylserine to Sec15. *EMBO J.* **32**, 874-885.

**de Graaf, P., Zwart, W. T., van Dijken, R. A., Deneka, M., Schulz, T. K., Geijsen, N., Coffer, P. J., Gadella, B. M., Verkleij, A. J., van der Sluijs, P. et al.** (2004). Phosphatidylinositol 4-kinasebeta is critical for functional association of rab11 with the Golgi complex. *Mol. Biol. Cell* **15**, 2038-2047.

**Deretic, D.** (2013). Crosstalk of Arf and Rab GTPases en route to cilia. *Small GTPases* **4**, 70-77.

**Deretic, D. and Mazelova, J.** (2009). Assay for in vitro budding of ciliary-targeted rhodopsin transport carriers. *Methods Cell Biol.* **94**, 241-257.

**Deretic, D. and Papermaster, D. S.** (1991). Polarized sorting of rhodopsin on post-Golgi membranes in frog retinal photoreceptor cells. *J. Cell Biol.* **113**, 1281-1293.

**Deretic, D., Huber, L. A., Ransom, N., Mancini, M., Simons, K. and Papermaster, D. S.** (1995). rab8 in retinal photoreceptors may participate in rhodopsin transport and in rod outer segment disk morphogenesis. *J. Cell Sci.* **108**, 215-224.

**Deretic, D., Traverso, V., Parkins, N., Jackson, F., Rodriguez de Turco, E. B. and Ransom, N.** (2004). Phosphoinositides, ezrin/moesin, and rac1 regulate fusion of rhodopsin transport carriers in retinal photoreceptors. *Mol. Biol. Cell* **15**, 359-370.

**Deretic, D., Williams, A. H., Ransom, N., Morel, V., Hargrave, P. A. and Arendt, A.** (2005). Rhodopsin C terminus, the site of mutations causing retinal disease, regulates trafficking by binding to ADP-ribosylation factor 4 (ARF4). *Proc. Natl. Acad. Sci. USA* **102**, 3301-3306.

**Eathiraj, S., Mishra, A., Prekeris, R. and Lambright, D. G.** (2006). Structural basis for Rab11-mediated recruitment of FIP3 to recycling endosomes. *J. Mol. Biol.* **364**, 121-135.

**Emmer, B. T., Maric, D. and Engman, D. M.** (2010). Molecular mechanisms of protein and lipid targeting to ciliary membranes. *J. Cell Sci.* **123**, 529-536.

**Feng, S., Knödler, A., Ren, J., Zhang, J., Zhang, X., Hong, Y., Huang, S., Peränen, J. and Guo, W.** (2012). A Rab8 guanine nucleotide exchange factor-effector interaction network regulates primary ciliogenesis. *J. Biol. Chem.* **287**, 15602-15609.

**Fielding, A. B., Schonteich, E., Matheson, J., Wilson, G., Yu, X., Hickson, G. R., Srivastava, S., Baldwin, S. A., Prekeris, R. and Gould, G. W.** (2005). Rab11-FIP3 and FIP4 interact with Arf6 and the exocyst to control membrane traffic in cytokinesis. *EMBO J.* **24**, 3389-3399.

**Fliegauf, M., Benzing, T. and Omran, H.** (2007). When cilia go bad: cilia defects and ciliopathies. *Nat. Rev. Mol. Cell Biol.* **8**, 880-893.

**Follit, J. A., Li, L., Vucica, Y. and Pazour, G. J.** (2010). The cytoplasmic tail of fibrocystin contains a ciliary targeting sequence. *J. Cell Biol.* **188**, 21-28.

**Follit, J. A., San Agustin, J. T., Jonassen, J. A., Huang, T., Rivera-Perez, J. A., Tremblay, K. D. and Pazour, G. J.** (2014). Arf4 is required for Mammalian development but dispensable for ciliary assembly. *PLoS Genet.* **10**, e1004170.

**Garcia-Gonzalo, F. R. and Reiter, J. F.** (2012). Scoring a backstage pass: mechanisms of ciliogenesis and ciliary access. *J. Cell Biol.* **197**, 697-709.

**Geng, L., Okuhara, D., Yu, Z., Tian, X., Cai, Y., Shibazaki, S. and Somlo, S.** (2006). Polycystin-2 traffics to cilia independently of polycystin-1 by using an N-terminal RVxP motif. *J. Cell Sci.* **119**, 1383-1395.

**Gerdes, J. M., Davis, E. E. and Katsanis, N.** (2009). The vertebrate primary cilium in development, homeostasis, and disease. *Cell* **137**, 32-45.

**Goldstein, O., Kukekova, A. V., Aguirre, G. D. and Acland, G. M.** (2010). Exonic SINE insertion in STK38L causes canine early retinal degeneration (erd). *Genomics* **96**, 362-368.

**Hales, C. M., Griner, R., Hobdy-Henderson, K. C., Dorn, M. C., Hardy, D., Kumar, R., Navarre, J., Chan, E. K., Lapierre, L. A. and Goldenring, J. R.** (2001). Identification and characterization of a family of Rab11-interacting proteins. *J. Biol. Chem.* **276**, 39067-39075.

**Hattula, K., Furuhjelm, J., Arffman, A. and Peränen, J.** (2002). A Rab8-specific GDP/GTP exchange factor is involved in actin remodeling and polarized membrane transport. *Mol. Biol. Cell* **13**, 3268-3280.

**Hickson, G. R., Matheson, J., Riggs, B., Maier, V. H., Fielding, A. B., Prekeris, R., Sullivan, W., Barr, F. A. and Gould, G. W.** (2003). Arfophilins are dual Arf/Rab 11 binding proteins that regulate recycling endosome distribution and are related to Drosophila nuclear fallout. *Mol. Biol. Cell* **14**, 2908-2920.

**Horgan, C. P., Oleksy, A., Zhdanov, A. V., Lall, P. Y., White, I. J., Khan, A. R., Futter, C. E., McCaffrey, J. G. and McCaffrey, M. W.** (2007). Rab11-FIP3 is critical for the structural integrity of the endosomal recycling compartment. *Traffic* **8**, 414-430.

**Inoue, H., Ha, V. L., Prekeris, R. and Randazzo, P. A.** (2008). Arf GTPase-activating protein ASAP1 interacts with Rab11 effector FIP3 and regulates pericentrosomal localization of transferrin receptor-positive recycling endosome. *Mol. Biol. Cell* **19**, 4224-4237.

**Jenkins, P. M., Hurd, T. W., Zhang, L., McEwen, D. P., Brown, R. L., Margolis, B., Verhey, K. J. and Martens, J. R.** (2006). Ciliary targeting of olfactory CNG channels requires the CNGB1b subunit and the kinesin-2 motor protein, KIF17. *Curr. Biol.* **16**, 1211-1216.

**Jian, X., Brown, P., Schuck, P., Gruschus, J. M., Balbo, A., Hinshaw, J. E. and Randazzo, P. A.** (2009). Autoinhibition of Arf GTPase-activating protein activity by the BAR domain in ASAP1. *J. Biol. Chem.* **284**, 1652-1663.

**Jing, J., Tarbutton, E., Wilson, G. and Prekeris, R.** (2009). Rab11-FIP3 is a Rab11-binding protein that regulates breast cancer cell motility by modulating the actin cytoskeleton. *Eur. J. Cell Biol.* **88**, 325-341.

**Junutula, J. R., Schonteich, E., Wilson, G. M., Peden, A. A., Scheller, R. H. and Prekeris, R.** (2004). Molecular characterization of Rab11 interactions with members of the family of Rab11-interacting proteins. *J. Biol. Chem.* **279**, 33430-33437.

**Kim, J., Lee, J. E., Heynen-Genel, S., Suyama, E., Ono, K., Lee, K., Ideker, T., Aza-Blanc, P. and Gleeson, J. G.** (2010). Functional genomic screen for modulators of ciliogenesis and cilium length. *Nature* **464**, 1048-1051.

**Knodler, A., Feng, S., Zhang, J., Zhang, X., Das, A., Peranen, J. and Guo, W.** (2010). Coordination of Rab8 and Rab11 in primary ciliogenesis. *Proc. Natl. Acad Sci. USA* **107**, 6346–6351.

**Lodowski, K. H., Lee, R., Ropelewski, P., Nemet, I., Tian, G. and Imanishi, Y.** (2013). Signals governing the trafficking and mistrafficking of a ciliary GPCR, rhodopsin. *J. Neurosci.* **33**, 13621-13638.

**Mazelova, J., Astuto-Gribble, L., Inoue, H., Tam, B. M., Schonteich, E., Prekeris, R., Moritz, O. L., Randazzo, P. A. and Deretic, D.** (2009). Ciliary targeting motif VxPx directs assembly of a trafficking module through Arf4. *EMBO J.* **28**, 183-192.

**Moritz, O. L., Tam, B. M., Hurd, L. L., Peränen, J., Deretic, D. and Papermaster, D. S.** (2001). Mutant rab8 impairs docking and fusion of rhodopsin-bearing post-Golgi membranes and causes cell death of transgenic Xenopus rods. *Mol. Biol. Cell* **12**, 2341-2351.

**Nachury, M. V., Loktev, A. V., Zhang, Q., Westlake, C. J., Peränen, J., Merdes, A., Slusarski, D. C., Scheller, R. H., Bazan, J. F., Sheffield, V. C. et al.** (2007). A core complex of BBS proteins cooperates with the GTPase Rab8 to promote ciliary membrane biogenesis. *Cell* **129**, 1201-1213.

**Nachury, M. V., Seeley, E. S. and Jin, H.** (2010). Trafficking to the ciliary membrane: how to get across the periciliary diffusion barrier? *Annu. Rev. Cell Dev. Biol.* **26**, 59-87.

**Nie, Z., Hirsch, D. S., Luo, R., Jian, X., Stauffer, S., Cremesti, A., Andrade, J., Lebowitz, J., Marino, M., Ahvazi, B. et al.** (2006). A BAR domain in the N terminus of the Arf GAP ASAP1 affects membrane structure and trafficking of epidermal growth factor receptor. *Curr. Biol.* **16**, 130-139.

**Pearring, J. N., Salinas, R. Y., Baker, S. A. and Arshavsky, V. Y.** (2013). Protein sorting, targeting and trafficking in photoreceptor cells. *Prog. Retin. Eye Res.* **36**, 24-51.

**Peter, B. J., Kent, H. M., Mills, I. G., Vallis, Y., Butler, P. J., Evans, P. R. and McMahon, H. T.** (2004). BAR domains as sensors of membrane curvature: the amphiphysin BAR structure. *Science* **303**, 495-499.

**Prekeris, R., Klumperman, J. and Scheller, R. H.** (2000). A Rab11/Rip11 protein complex regulates apical membrane trafficking via recycling endosomes. *Mol. Cell* **6**, 1437-1448.

**Prekeris, R., Davies, J. M. and Scheller, R. H.** (2001). Identification of a novel Rab11/25 binding domain present in Eferin and Rip proteins. *J. Biol. Chem.* **276**, 38966-38970.

**Randazzo, P. A., Andrade, J., Miura, K., Brown, M. T., Long, Y. Q., Stauffer, S., Roller, P. and Cooper, J. A.** (2000). The Arf GTPase-activating protein ASAP1 regulates the actin cytoskeleton. *Proc. Natl. Acad. Sci. USA* **97**, 4011-4016.

**Sang, L., Miller, J. J., Corbit, K. C., Giles, R. H., Brauer, M. J., Otto, E. A., Baye, L. M., Wen, X., Scales, S. J., Kwong, M. et al.** (2011). Mapping the NPHP-JBTS-MKS protein network reveals ciliopathy disease genes and pathways. *Cell* **145**, 513-528.

**Schiel, J. A., Simon, G. C., Zaharris, C., Weisz, J., Castle, D., Wu, C. C. and Prekeris, R.** (2012). FIP3-endosome-dependent formation of the secondary ingression mediates ESCRT-III recruitment during cytokinesis. *Nat. Cell Biol.* **14**, 1068-1078.

**Schonteich, E., Pilli, M., Simon, G. C., Matern, H. T., Junutula, J. R., Sentz, D., Holmes, R. K. and Prekeris, R.** (2007). Molecular characterization of Rab11-FIP3 binding to ARF GTPases. *Eur. J. Cell Biol.* **86**, 417-431.

**Shin, O. H., Ross, A. H., Mihai, I. and Exton, J. H.** (1999). Identification of arfophilin, a target protein for GTP-bound class II ADP-ribosylation factors. *J. Biol. Chem.* **274**, 36609-36615.

**Singla, V. and Reiter, J. F.** (2006). The primary cilium as the cell's antenna: signaling at a sensory organelle. *Science* **313**, 629-633.

**Söderberg, O., Gullberg, M., Jarvius, M., Ridderstråle, K., Leuchowius, K. J., Jarvius, J., Wester, K., Hydbring, P., Bahram, F., Larsson, L. G. et al.** (2006). Direct observation of individual endogenous protein complexes in situ by proximity ligation. *Nat. Methods* **3**, 995-1000.

**Trifilieff, P., Rives, M. L., Urizar, E., Piskorowski, R. A., Vishwasrao, H. D., Castrillon, J., Schmauss, C., Slättman, M., Gullberg, M. and Javitch, J. A.** (2011). Detection of antigen interactions ex vivo by proximity ligation assay: endogenous dopamine D2-adenosine A2A receptor complexes in the striatum. *Biotechniques* **51**, 111-118.

**Trivedi, D. and Williams, D. S.** (2010). Ciliary transport of opsin. *Adv. Exp. Med. Biol.* **664**, 185-191.

**Trivedi, D., Colin, E., Louie, C. M. and Williams, D. S.** (2012). Live-cell imaging evidence for the ciliary transport of rod photoreceptor opsin by heterotrimeric kinesin-2. *J. Neurosci.* **32**, 10587-10593.

**Valente, E. M., Rosti, R. O., Gibbs, E. and Gleeson, J. G.** (2014). Primary cilia in neurodevelopmental disorders. *Nat. Rev. Neurol.* **10**, 27-36.

**Wang, J. and Deretic, D.** (2014). Molecular complexes that direct rhodopsin transport to primary cilia. *Prog. Retin. Eye Res.* **38**, 1-19.

**Wang, J., Morita, Y., Mazelova, J. and Deretic, D.** (2012). The Arf GAP ASAP1 provides a platform to regulate Arf4- and Rab11-Rab8-mediated ciliary receptor targeting. *EMBO J.* **31**, 4057-4071.

**Ward, H. H., Brown-Glaberman, U., Wang, J., Morita, Y., Alper, S. L., Bedrick, E. J., Gattone, V. H., I. I, Deretic, D. and Wandinger-Ness, A.** (2011). A conserved signal and GTPase complex are required for the ciliary transport of polycystin-1. *Mol. Biol. Cell* **22**, 3289-3305.

**Westlake, C. J., Baye, L. M., Nachury, M. V., Wright, K. J., Ervin, K. E., Phu, L., Chalouni, C., Beck, J. S., Kirkpatrick, D. S., Slusarski, D. C. et al.** (2011). Primary cilia membrane assembly is initiated by Rab11 and transport protein particle II (TRAPPII) complex-dependent trafficking of Rabin8 to the centrosome. *Proc. Natl. Acad. Sci. USA* **108**, 2759-2764.

**Wilson, G. M., Fielding, A. B., Simon, G. C., Yu, X., Andrews, P. D., Hames, R. S., Frey, A. M., Peden, A. A., Gould, G. W. and Prekeris, R.** (2005). The FIP3-Rab11 protein complex regulates recycling endosome targeting to the cleavage furrow during late cytokinesis. *Mol. Biol. Cell* **16**, 849-860.

**Yoshimura, S., Egerer, J., Fuchs, E., Haas, A. K. and Barr, F. A.** (2007). Functional dissection of Rab GTPases involved in primary cilium formation. *J. Cell Biol.* **178**, 363-369.